

The Crystal Structure of α -La₂Mo₂O₉ and the Structural Origin of the Oxide Ion Migration Pathway

Ivana Radosavljevic Evans,* Judith A. K. Howard, and John S. O. Evans

Department of Chemistry, University of Durham, Science Site, South Road,
Durham DH1 3LE, United Kingdom

Received January 10, 2005. Revised Manuscript Received May 12, 2005

We describe for the first time the full 3D atomic structure of room-temperature α -La₂Mo₂O₉. The material, despite its simple chemical formula, has a remarkable 312 crystallographically unique atoms and is thus one of the most complex oxide structures reported to date. Despite this complexity, the structural results offer significant insight into the O²⁻ migration pathway in the anion conducting high-temperature form, β -La₂Mo₂O₉. The material contains a mixture of 4, 5, and 6 coordinated Mo sites, suggesting that variable Mo coordination number is a key factor in providing a low-energy O²⁻ conduction pathway. We provide quantitative analysis showing that the positions in the ordered array of 216 oxygen sites of α -La₂Mo₂O₉ are directly related to the average sites occupied in β -La₂Mo₂O₉, providing compelling evidence that the high-temperature conducting form of the material has a time-averaged version of the low-temperature structure.

Introduction

Oxide ion conductors are technologically important materials, essential for applications including oxygen sensors and pumps, membranes for oxygen separation, and solid oxide fuel cells.^{1–3} Currently, the most commonly used materials are based on stabilized zirconia; however, one of the main limiting factors associated with their use is their relatively low oxide ion conductivity below 1000 °C. Much of the research carried out in this field has therefore been focused on the search for materials with high conductivity at lower operating temperatures. Potentially exploitable oxide ion conductors have been identified in a few different structural families, such as the Aurivillius type phases, fluorites, perovskites, pyrochlores, and brownmillerites, as well as the recently developed LAMOX materials based on lanthanum molybdate, La₂Mo₂O₉.

Exceptional oxide ion conductivity in La₂Mo₂O₉, with $\sigma = 6 \times 10^{-2} \text{ Scm}^{-1}$ at 800 °C, has been reported by Lacorre et al.,⁴ they also reported that this high conductivity is associated with a phase transition from the room-temperature α -form to a high-temperature β -form at 580 °C, which is accompanied by a rise in conductivity of almost 2 orders of magnitude.⁵

La₂Mo₂O₉ was first synthesized by Fournier et al.,⁶ who prepared it by conventional solid-state techniques. Since the

resurgence of research interest in this material owing to its outstanding properties, it has also been prepared by mechanochemical synthesis,⁷ sol–gel routes,⁸ and from freeze-dried precursors.⁹ None of these methods have hitherto yielded single crystals suitable for structural characterization. Numerous substitutions into La₂Mo₂O₉ have been successfully carried out at both the cation sites and oxygen sites: (La_{2-x}M_x)Mo₂O_{9-y}, M = Sr, Ba, K, Bi;¹⁰ (La_{2-x}R_x)Mo₂O₉, R = Nd, Gd, Y;¹¹ La₂(Mo_{2-x}M_x)₂O₉, M = Re, S, W, Cr, V;¹⁰ and La₂Mo₂O_{9-1/2x}F_x¹² have all been prepared. In most cases, the high-temperature simple cubic β -La₂Mo₂O₉ structure is stabilized to room temperature, the phase transition to the α -form being suppressed. Notable exceptions are Nd-doped phases which adopt the monoclinic structure throughout the substitution range and the fluorinated phases, which appear to crystallize in the α -form for $x = 0.10$ but adopt a different type of superstructure for higher doping levels. Despite the discovery of these various doped systems with related structures, the structure of the parent material, α -La₂Mo₂O₉, has so far remained unsolved.

Structural insight into α -La₂Mo₂O₉ is important for several reasons. Firstly, in a recent publication,¹³ Subasri et al. have questioned the magnitude and nature of conduction originally reported for La₂Mo₂O₉. Without a detailed understanding of the structure of the low-temperature α -phase, resolving such issues has been difficult, though recent studies confirmed

* Author to whom correspondence should be addressed. Fax: +44 191 384737; tel: +44 191 334 2004; e-mail: ivana.radosavljevic@durham.ac.uk.

(1) Maskell, W. C. *Solid State Ionics* **2000**, *134*, 43.

(2) Mairesse, G. C. R. *Acad. Sci., Ser. IIc* **1999**, *2*, 651.

(3) Huang, K.; Wan, J.; Goodenough, J. B. *J. Mater. Sci.* **2001**, *36*, 5, 1093.

(4) Lacorre, P.; Goutenoire, F.; Bohnke, O.; Retoux, R.; Lalignat, Y. *Nature* **2000**, *404*, 856.

(5) Goutenoire, F.; Isnard, O.; Retoux, R.; Lacorre, P. *Chem. Mater.* **2000**, *12*, 2575.

(6) Fournier, J. P.; Fournier, J.; Kohlmuller, R. *Bull. Soc. Chim. Fr.* **1970**, 4277.

(7) Lacorre, P.; Retoux, R. *J. Solid State Chem.* **1997**, *132*, 443.

(8) Kuang, W.; Fan, Y.; Yao, K.; Chen, Y. *J. Solid State Chem.* **1998**, *140*, 354.

(9) Marrero-Lopez, D.; Ruiz-Morales, J. C.; Nunez, P.; Abrantes, J. C. C.; Frade, J. R. *J. Solid State Chem.* **2004**, *177*, 2377.

(10) Goutenoire, F.; Isnard, O.; Suard, E.; Bohnke, O.; Lalignat, Y.; Retoux, R.; Lacorre, P. *J. Mater. Chem.* **2001**, *11*, 119.

(11) Georges, S.; Goutenoire, F.; Altorfer, F.; Sheptyakov, D.; Fauth, F.; Suard, E.; Lacorre, P. *Solid State Ionics* **2003**, *161*, 231.

(12) Arulraj, A.; Goutenoire, F.; Tabellout, M.; Bohnke, O.; Lacorre, P. *Chem. Mater.* **2002**, *14*, 2492.

(13) Subasri, R.; Nafe, H.; Aldinger, F. *Mater. Res. Bull.* **2003**, *38*, 1965.

Table 1: Crystallographic Details for α -La₂Mo₂O₉

formula	α -La ₂ Mo ₂ O ₉
MW	613.69
crystal system	monoclinic
space group	P2 ₁
<i>a</i> (Å)	14.325(3)
<i>b</i> (Å)	21.482(4)
<i>c</i> (Å)	28.585(6)
β (°)	90.40(3) ^o
<i>V</i> (Å ³)	8796(3)
<i>Z</i>	48
density (g/cm ⁻³)	5.561
μ (mm ⁻¹)	14.8
# unique reflections	27496
<i>I</i> / σ cutoff	3
# observed reflections	19233
# parameters refined	1730
<i>R</i> (%)	8.80
<i>wR</i> (%)	8.78

the oxide ion conducting properties.¹⁴ Secondly, following the discovery of the LAMOX family, the lone-pair substitution (LPS) concept has been proposed as a new approach to making new oxide ion conductors from known compounds,¹⁵ on the basis of controlled isovalent or aliovalent substitution of the lone-pair cation. It is, therefore, important to gain a better insight into how such a substitution affects the structure and the resulting properties of the material obtained. The successful elucidation of the room-temperature structure of La₂Mo₂O₉ in this work allows the study of such relationships by comparative analysis of the β -SnWO₄, high-temperature β -La₂Mo₂O₉, and low-temperature α -La₂Mo₂O₉ structures.

Experimental Section

A polycrystalline sample of La₂Mo₂O₉ was prepared from stoichiometric amounts of La₂O₃ and MoO₃. The reactants were intimately ground, heated at a rate of 10°/min to 900 °C, and held at this temperature for 3 days with intermediate grinding. A small amount of the La₂Mo₂O₉ obtained was melted in an alumina crucible, cooled at a rate of 3°/min to 300 °C, and then furnace-cooled to room temperature. Very small clear crystals were isolated from the cooled melt.

Single-crystal X-ray diffraction experiments were carried out on a Bruker SMART three-circle diffractometer equipped with an APEX CCD detector and a Bede Microsource X-ray source of Mo K α radiation. A cube-shaped crystal of approximate dimensions 0.04 × 0.04 × 0.04 mm³ was used. A full sphere of data was collected with a counting time of 40 s per frame. A multiscan absorption correction was applied to the raw data and the resulting *R*_{int} was 2.8%. Frames were integrated using the program SAINT, and data reduction was carried out using XPREP.¹⁶ The crystal structure was solved by direct methods implemented in the program SIR92¹⁷ and was refined by full-matrix least squares against *F* in the Crystals suite.¹⁸ The Flack parameter for this polar structure refined to 0.11(7) and was therefore removed for final cycles of refinement. Crystallographic details are given in Table 1 and a crystallographic information file (CIF) has been deposited.

Structure Solution of α -La₂Mo₂O₉. Our single-crystal X-ray diffraction studies of α -La₂Mo₂O₉ show that at room temperature all reflections could be indexed using a monoclinic cell, with unit cell parameters *a* = 14.325(3) Å, *b* = 21.482(4) Å, *c* = 28.585(6) Å, and β = 90.40(3)^o and space group P2₁. This 2 × 3 × 4 superstructure relative to the cubic high-temperature β form and a small monoclinic distortion has also been suggested by electron diffraction and neutron diffraction observations published previously.⁵ The cell metric is also consistent with peak splitting observed in time-of-flight neutron powder diffraction patterns (see Supplementary Information). Given the cell metric and symmetry, the crystal structure of α -La₂Mo₂O₉ contains a remarkable 312 crystallographically independent atoms: 48 La, 48 Mo, and 216 O. The structure was solved by a combination of direct methods, used to locate the metal sites, and difference Fourier maps that revealed the oxygen atom positions. The final model was obtained by anisotropic refinement of cations and isotropic treatment of oxygen atoms and gave agreement factors of *R* = 8.80% and *wR* = 8.78%. Full atomic coordinates and refinement details have been deposited as Supplementary Information.

The structure of α -La₂Mo₂O₉ is far from that of a “typical” inorganic oxide. The 312 atoms in the asymmetric unit make it the second largest oxide structure solved by single-crystal methods in the 2004 issue of ICSD¹⁹ (the first and the third containing 441 and 105 unique atoms, respectively); when deposited, it will be the sixth largest structure of any type in the ICSD. In many ways, the structure complexity is closer to that of a small protein than a normal inorganic material, and it is important to assess the quality and uniqueness of the solution in that light.

A first indication of the quality of the refinement is given by the range of the atomic displacement parameters, with min/max/average/esd of *U*_{equiv}/*U*_{iso} values for La, Mo, and O sites of 0.009/0.067/0.020/0.01, 0.010/0.045/0.017/0.007, and 0.009/0.11/0.04/0.02 Å², respectively. The values are thus all within the range expected for materials of this type. Bond valence sums²⁰ have also been calculated (see Figure 2, supplementary data) to assess the quality of the refinement. It should, however, be realized that for a structure this complex, in which the scatter is dominated by La/Mo sites, the uncertainty on individual M–O bond lengths is relatively large. This in turn leads to an uncertainty in individual bond valence sums of up to half a unit. When bond length uncertainties are propagated into bond valence calculations as uncorrelated errors, the spread of bond valence sums is such that all observations are within 3 standard uncertainties from the expected values of 3 and 6 for La and Mo sites, respectively (see Supplementary Information).

To assess the sensitivity of the data to small variations in atomic arrangements, we have developed methods for simultaneously refining against single-crystal data and bond valence summation restraints and have refined our model²¹ against both sets of observations. Restraints were weighed such that individual La valence sums ranged from 2.94 to 3.17 and Mo from 5.99 to 6.05, that is, a narrower range than one might expect to find in practice. In the resultant model, atomic coordinates differ by an average of 0.076 Å from those obtained by conventional unrestrained refinement, and the largest shift of any atom was 0.173 Å. Given the average standard uncertainties on the oxygen coordinates in the freely refined structure (0.0027/0.0019/0.0016 for *x/y/z* coordinates), a shift of one esd in *x/y/z* would correspond to a distance of ~0.073 Å (essentially identical to the average shift of atoms between these models). We conclude that a restrained model with statistically insignificant shifts in coordinates from the freely refined one gives

(14) Marrero-Lopez, D.; Ruiz-Morales, J. C.; Perez-Coll, D.; Nunez, P.; Abrantes, J. C. C.; Frade, J. R. J. *Solid State Electrochem.* **2004**, *8*, 638.

(15) Lacorre, P. *Solid State Sci.* **2000**, *2*, 755.

(16) SAINT+, Release 6.22; Bruker Analytical Systems: Madison, WI, 1997–2001.

(17) Altomare, G.; Casciarano, G.; Giacovazzo, G. C.; Guagliardi, A.; Burla, M. C.; Polidori, G.; Camalli, M. *J. Appl. Crystallogr.* **1994**, *27*, 435.

(18) Betteridge, P. W.; Carruthers, J. R.; Cooper, R. I.; Prout K.; Watkin, D. J. *J. Appl. Crystallogr.* **2003**, *36*, 1487.

(19) ICSD, Fachinformationszentrum (FIZ) Karlsruhe, 2004.

(20) Brown I. D.; Altermatt D. *Acta Crystallogr.* **1985**, *B41*, 244.

(21) Evans, J. S. O.; Coelho, A. A. unpublished results.

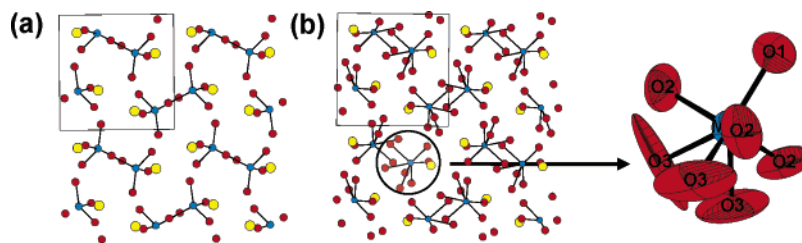


Figure 1. (a) Structure of β - SnWO_4 ; (b) structure of β - $\text{La}_2\text{Mo}_2\text{O}_9$; Sn/La atoms in yellow, W/Mo atoms in blue, O atoms in red. The coordination environment of the Mo site and atomic displacement parameters of oxygens in (b) are highlighted. The square represents one cubic unit cell. In β - SnWO_4 , there are isolated WO_4 tetrahedra; their apparent overlap in (a) is merely due to the perspective shown.

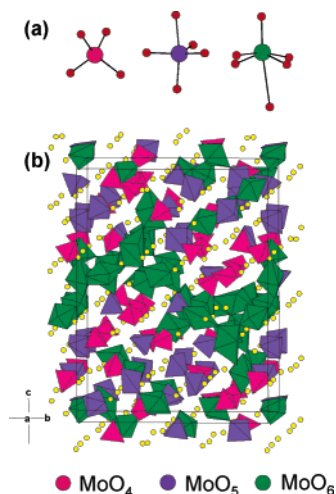


Figure 2. (a) Three Mo coordination geometry types observed in α - $\text{La}_2\text{Mo}_2\text{O}_9$, (b) Polyhedral representation of α - $\text{La}_2\text{Mo}_2\text{O}_9$: tetrahedral groups shown in pink, trigonal bipyramidal in purple, octahedral in green; yellow spheres represent La atoms.

bond valence sums in excellent agreement with those expected. Given the minor coordinate shifts, we choose to report the unrestrained structural model.

Because of the complexity of the structure, it is impossible to be as precise about individual oxygen atom parameters as one could be for a simple material. There remains a possibility that a small number of the 216 oxygen sites are partially disordered over two or more positions. This can perhaps be inferred from the slightly higher atomic displacement parameters for certain O sites; 8 of the 216 oxygen sites have U_{iso} values in the range of 0.09–0.11 \AA^2 . We do not feel that the data quality is sufficient to allow this possibility to be investigated further. However, the magnitude of the atomic displacement parameters suggests that the extent of any possible disorder is relatively low. Also, introduction of additional oxygen sites at random incorrect positions always results in an increase of the R factor and atomic displacement parameters refining to unreasonably high values, showing that the data are consistent with the oxygen arrangement reported. Finally, Rietveld fits show that the atomic model reported is also consistent with neutron powder diffraction data (see Supplementary Information).

Discussion of Structure and Implications for Oxide Ion Conductivity

The structural properties of $\text{La}_2\text{Mo}_2\text{O}_9$ at high temperature were first investigated by Goutenoire et al.^{5,11} by powder neutron diffraction. They found that above a phase transition at 580 $^\circ\text{C}$ β - $\text{La}_2\text{Mo}_2\text{O}_9$ is cubic. The high-temperature β -structure can be best understood by reference to the β - SnWO_4 structure; this can be appreciated by writing both materials with a general formula $\text{A}_2\text{B}_2\text{O}_{8+\delta}$ ($\delta = 1/0$,

respectively). β - SnWO_4 ²² has a cubic structure in which Sn and W lie on threefold axes and form a metal sublattice such that each cation is surrounded by seven cations of the other type at about 4 \AA . O atoms create a distorted octahedral coordination around Sn, while W atoms are found in regular, isolated WO_4 tetrahedral groups. The relationship between β - $\text{La}_2\text{Mo}_2\text{O}_9$ and β - SnWO_4 is such that the metal arrangement in the two structures is essentially the same, with the main differences between the two phases arising from the rearrangement of oxygen atoms which accompanies the change in oxygen stoichiometry. In β - SnWO_4 , there are two fully occupied oxygen sites, one on the threefold axis and one on a general position. In β - $\text{La}_2\text{Mo}_2\text{O}_9$, there are three unique oxygen atoms: a fully occupied O1 position on the threefold axis and two disordered partially occupied sites: a preferentially occupied O2 site approximately in the equatorial plane of the cation perpendicular to the threefold axis and a less occupied O3; both sites have large atomic displacement parameters (at 670 $^\circ\text{C}$, fractional occupancies are 0.78(2) and 0.38(2) and U_{equiv} values 0.097(5) and 0.24(2) \AA^2 for the two sites¹¹).

In the α - $\text{La}_2\text{Mo}_2\text{O}_9$ crystal structure, the basic cation arrangement of β - SnWO_4 is preserved and the major differences are found in the oxygen sublattice. The shifts of cations relative to the ideal β - SnWO_4 structure are fairly small, the average values being 0.35 and 0.28 \AA for La and Mo relative to Sn and W, respectively. The displacements within the oxygen sublattice are much larger, with an average distance between any given O atom in α - $\text{La}_2\text{Mo}_2\text{O}_9$ and the nearest O site in the ideal β - SnWO_4 structure of 0.69 \AA .

Sn in β - SnWO_4 exists in a distorted octahedral coordination. There are three short bonds at 2.21 \AA and three long ones at 2.81 \AA ; this type of arrangement can be viewed as typical for a cation with a stereochemically active lone pair of electrons. In α - $\text{La}_2\text{Mo}_2\text{O}_9$, however, this site is occupied by a large, closed-subshell cation La^{3+} , and a change of coordination type to higher coordination numbers and irregular geometries occur. Crystallographically unique La atoms have a coordination shell containing between 6 and 12 oxygen atoms, with 30 out of the 48 independent La atoms being nine-coordinate.

The Mo atoms in α - $\text{La}_2\text{Mo}_2\text{O}_9$ are found in three different basic coordination types: there are 15 tetrahedral, 15 trigonal bipyramidal, and 18 octahedral Mo atoms. Three typical local coordinations are shown in Figure 2a. The six-coordinate Mo atoms typically contain one bond significantly longer

than the others, as commonly seen in some other d^0 systems, such as the coordination of V in V_2O_5 .²³ A polyhedral representation of α - $\text{La}_2\text{Mo}_2\text{O}_9$ is shown in Figure 2b.

It is instructive to consider where the “extra” oxygen atoms in $\text{La}_2\text{Mo}_2\text{O}_9$ ($\text{A}_2\text{B}_2\text{O}_9$) are situated relative to β - SnWO_4 ($\text{A}_2\text{B}_2\text{O}_8$). Such analysis is somewhat complicated by the fact that the WO_4 groups occur as isolated tetrahedra in β - SnWO_4 , whereas there is significant oxygen cross-linking of MoO_n coordination polyhedra in α - $\text{La}_2\text{Mo}_2\text{O}_9$. For example, a local configuration of two B and eight O atoms could give rise to either two isolated BO_4 tetrahedra or a corner-sharing BO_5 trigonal bipyramid and BO_4 tetrahedron. Taking into account the sharing patterns of oxygen atoms within the three coordination types, the local “effective” oxygen coordination of the sites becomes 3.73, 4.77, and 4.94, for tetrahedra, trigonal bipyramids, and octahedra, respectively. This suggests that, relative to the W coordination number of four in the lone pair containing parent phase β - SnWO_4 , there is a net effective oxygen content increase at the five- and six-coordinate Mo sites in α - $\text{La}_2\text{Mo}_2\text{O}_9$. The color coding of Figure 2b therefore gives a direct indication as to the location of excess oxygen.

To understand the oxide ion conduction mechanism in this material, it is also important to compare the oxygen distribution in α - $\text{La}_2\text{Mo}_2\text{O}_9$ to that in the high-temperature β form. Figure 3 shows the oxygen coordination of the B site in β - SnWO_4 , β - $\text{La}_2\text{Mo}_2\text{O}_9$, and α - $\text{La}_2\text{Mo}_2\text{O}_9$.

From Figure 3, there is a clear correlation between the dynamically disordered oxygen distribution in β - $\text{La}_2\text{Mo}_2\text{O}_9$ and the static O distribution in room-temperature α - $\text{La}_2\text{Mo}_2\text{O}_9$. This can be appreciated qualitatively from the positions and numbers of independent O atoms in α - $\text{La}_2\text{Mo}_2\text{O}_9$ relative to the shapes of oxygen atomic displacement parameters and site fractional occupancies in β - $\text{La}_2\text{Mo}_2\text{O}_9$. To quantify the relationship, we have subdivided the 216 unique oxygen atoms in the α structure into those that lie

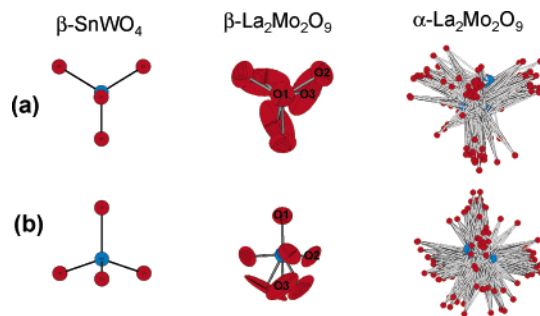


Figure 3. Comparison of B site coordination in β - SnWO_4 ,¹⁶ β - $\text{La}_2\text{Mo}_2\text{O}_9$,¹¹ and α - $\text{La}_2\text{Mo}_2\text{O}_9$; (a) and (b) show two mutually perpendicular views. For α - $\text{La}_2\text{Mo}_2\text{O}_9$, the picture represents a superposition of all independent Mo atoms and their coordination spheres obtained by transformation of the monoclinic superstructure into the underlying cubic subcell.

closest to each of the three crystallographic sites used to model the disordered β structure. We find that there are 47, 116, and 53 oxygens that lie nearest to O1, O2, and O3 of β - $\text{La}_2\text{Mo}_2\text{O}_9$, respectively, which, taking site multiplicities into account, would correspond to fractional site occupancies in a simple cubic model of 0.33, 0.81, and 0.37; these are remarkably close to the experimentally determined occupancies for β - $\text{La}_2\text{Mo}_2\text{O}_9$ of 0.33, 0.78(2), and 0.38(2).¹¹

Our analysis thus provides compelling evidence that the structure of the oxide ion conducting phase corresponds to a time-averaged version of the room-temperature structure. In the context of an oxide ion conduction mechanism, the structural evidence presented here strongly suggests that the variable coordination environment possible for the Mo cation is key for producing the low-energy migration path for oxide ions.

Supporting Information Available: Time-of-flight neutron powder diffraction data and bond valence sums in the freely refined structure (PDF) as well as crystallographic data for α - $\text{La}_2\text{Mo}_2\text{O}_9$ (CIF).

(23) Enjalbert, R.; Galy, J. *Acta Crystallogr.* **1986**, C42, 1467.